Arch. Metall. Mater., Vol. 61 (2016), No 1, p. 9–12

DOI: 10.1515/amm-2016-0006

B. ZHANG*,**, H. WAGNER**,***, M. BÜCHSENSCHÜTZ-GÖBELER**, Y. LUO**, S. KÜCHEMANN**, W. ARNOLD**,****,#, K. SAMWER**

MEASUREMENT OF THE INDENTATION MODULUS AND THE LOCAL INTERNAL FRICTION IN AMORPHOUS SiO_2 USING ATOMIC FORCE ACOUSTIC MICROSCOPY

Abstract. For the past two decades, atomic force acoustic microscopy (AFAM), an advanced scanning probe microscopy technique, has played a promising role in materials characterization with a good lateral resolution at micro/nano dimensions. AFAM is based on inducing out-of-plane vibrations in the specimen, which are generated by an ultrasonic transducer. The vibrations are sensed by the AFM cantilever when its tip is in contact with the material under test. From the cantilver's contact-resonance spectra, one determines the real and the imaginary part of the contact stiffness k^*, and then from these two quantities the local indentation modulus M' and the local damping factor Q_{loc}^{-1} can be obtained with a spatial resolution of less than 10 nm. Here, we present measured data of M' and of Q_{loc}^{-1} for the insulating amorphous material, a-SiO_2. The amorphous SiO_2 layer was prepared on a crystalline Si wafer by means of thermal oxidation. There is a spatial distribution of the indentation modulus M' and of the internal friction Q_{loc}^{-1}. This is a consequence of the potential energy landscape for amorphous materials.

Keywords: Amorphous materials, potential energy landscape, internal friction, atomic force acoustic microscopy

1. Introduction

Internal friction or ultrasonic attenuation in solids is caused by the interaction of elastic stress-fields with elementary excitations in the solids such as phonons, electrons, magnons, lattice defects like dislocations, diffusion of interstitials and impurities, just to name a few [1]. In case of solids with a micro-, nano- or an amorphous structure, new paths are opened for the interaction with oscillatory stress-fields by scattering at grain boundaries and/or structural relaxation. In case the linear size of the microstructure becomes comparable to the wavelength employed or to the size of the stress field, additional effects occur. It is of special interest to study the interactions not only globally, but also locally, in order to learn more about the distribution of relaxation strengths in an amorphous structure. Here, we report data for a-SiO_2 as an extension of our earlier work for a-PdCuSi [2].

2. Atomic force microscopy – contact resonances

In atomic force microscopy a cantilever is employed as sensor. It exhibits many modes depending on its shape and geometrical dimensions. Their resonance frequencies cover a wide frequency spectrum extending into the ultrasonic frequency range also used for internal friction measurements. There are a number of atomic force techniques which combine the cantilever dynamics with ultrasonics, see for examples the collected papers in Ref. [3].

AFAM allows to measure the local indentation modulus M' by determining first the contact stiffness k^* and then relating this quantity to M' using a suitable mechanical model. The modulus M' is an elastic constant which accounts for the compressive and the shear deformations in the tip-sample contact zone with the isotropic or anisotropic material [4]. Due to the damping of the oscillating cantilever, the contact stiffness $k^* = k_r + ik_i$ becomes complex and hence the indentation modulus as well. For a circular contact this can be expressed as:

$$k_r = 2a_c \times M' \tag{1a}$$

$$k_i = 2a_c \times M'', \tag{1b}$$

where the complex indentation modulus is $M = M' + iM''$ and a_c is the contact radius. Because the cantilever is excited dynamically, viscoelastic damping yields for the imaginary part of the contact stiffness $k_i = \omega \times \gamma$ [5], where γ is the damping in the contact zone. Formally, the damping is represented by a dash-pot parallel to a spring which stands for the real part of the contact stiffness, k_r. The local contact damping Q_{loc}^{-1} is then given by

* SCHOOL OF MATERIALS SCIENCE AND ENGINEERING, HEFEI UNIVERSITY OF TECHNOLOGY, TUNXI ROAD 193, HEFEI 230009, ANHUI PROVINCE, P. R. CHINA

** 1. PHYSIKALISCHES INSTITUT, GEORG-AUGUST UNIVERSITÄT, FRIEDRICH-HUND-PLATZ 1, D-37077 GÖTTINGEN, GERMANY

*** DEPARTMENT OF MECHANICAL ENGINEERING, MASSACHUSETTS INSTITUTE OF TECHNOLOGY, 77 MASSACHUSETTS AVENUE, CAMBRIDGE, MA 02139-4307, USA

**** DEPARTMENT OF MATERIALS AND MATERIALS TECHNOLOGY, SAARLAND UNIVERSITY, CAMPUS D 2.2, D-66123 SAARBRÜCKEN, GERMANY

Corresponding author: w.arnold@mx.uni-saarland.de

$$Q_{loc}^{-1} = \frac{k_i}{k_r} = \frac{\omega\gamma}{k_r} = \frac{M''}{M'} . \qquad (2)$$

Neither k_r nor k_i are directly measurable. The experimental quantities accessible are the resonance frequencies f_{res} and the Q-value of the contact resonance $Q_{res}^{-1} = \Delta f_{res}/f_{res}$ where Δf_{res} is the width of the resonance curve. To what extent Q_{loc}^{-1} contributes to Q_{res}^{-1} is determined by the local velocity $\partial y/\partial t$ of the cantilever at the tip position. How to evaluate the local indentation modulus and the local internal friction Q_{loc}^{-1} has been discussed in a number of recent papers, see for example [5, 6].

3. Experimental techniques

For the AFAM measurements, we used a Multimode AFM with a Nanoscope IV controller manufactured by Veeco-Metrology (now Bruker-Nano, S. Barbara, Ca.) and a commercial ultrasonic transducer (Panametrics V133-SM) with a center frequency of 2.25 MHz to excite the modes using the AFAM technique [2, 6]. In order to convert the measured contact stiffnesses into indentation moduli, calibration of the AFAM technique has to be undertaken [2]. Here, the mean value of the identation modulus of the amorphous metallic glass PdCuSi was used as a calibration material. Measurements were taken in maps on 100 different positions in a squared lattice of 200 × 200 nm^2 size. Two maps were taken for amorphous SiO_2 and from these maps corresponding statistics were derived. They were compared to data on the single crystal $SrTiO_3$. The 500 nm thick amorphous SiO_2 layer was prepared on a crystalline Si wafer by means of the thermal oxidation at 1100°C in air.

4. Experimental results

Figure 1a shows the distribution of the indentation modulus M' in amorphous SiO_2. The averaged value for all contact-resonance frequencies was f_{cont} = 1.678 MHz and the resonance frequency of the free cantilever was f_{fr} = 301 kHz. The difference between the maximal and the minimal frequency was 15 kHz. The shape of the curves was Lorentzian. From the measured contact-resonance frequencies, the contact stiffness was calculated [2]. It varied between 3140 - 3305 N/m which entails an indentation modulus M' of 47-52 GPa with an average value of 50 GPa. In the distribution of Fig. 1a, this corresponds to a variation of 2.9% relative to the average value. It is interesting to note that there is a tail in the distribution to lower moduli. For fused quartz, one expects an indentation modulus of 76 GPa [7]. Apparently, thermal oxidation of Si leads to an amorphous SiO_2 layer with an elastic modulus reduced appreciably in comparison to fused quartz. Comparison experiments with nano-indentation were made for the metallic glass PdCuSi at the time at the time when experiments reported here and earlier [2] were carried out. They yielded the same results within measurement accuracy [2] and this holds also for other measurements made using AFAM [7-10]. Measurement accuracy below 10% can be obtained by careful calibration procedures [7-10].

The influence of the surface roughness on the distribution of the indentation modulus of a-PdCuSi has been discussed in the supplementary information of Ref. [2] and it turned out to be negligible for our measurements. The conditions for the measurements on SiO_2 were the same [11] and we are confident that the interpretation of our data cannot be explained by surface roughness effects. If there are larger variations in surface roughness, it is possible to deconvolute the data in respect to surface roughness [9].

The variations in $\Delta M'/M'$ can be viewed as a spatially varying modulus defect. Therefore a corresponding variation must be seen in the internal friction as well. Based on the evaluation procedure discussed in [6], Fig. 1b shows the distribution of the local damping for amorphous SiO_2 with the maximum at $Q_{loc}^{-1} \approx 4.1\times10^{-2}$ and a distribution width of $\Delta Q_{loc}^{-1} \approx 6\times10^{-3}$ (full width) and hence $\Delta Q_{loc}^{-1}/Q_{loc}^{-1} \approx 0.15$. For comparison, we made the same type of measurements on the single crystal (100)-$SrTiO_3$ [2]. For $SrTiO_3$, the maximum of the distribution occurred at $Q_{loc}^{-1} \approx 7.7\times10^{-3}$ and the distribution width was $\Delta Q_{loc}^{-1} \approx 8\times10^{-4}$ and resulting in $\Delta Q_{loc}^{-1}/Q_{loc}^{-1} \approx 0.1$.

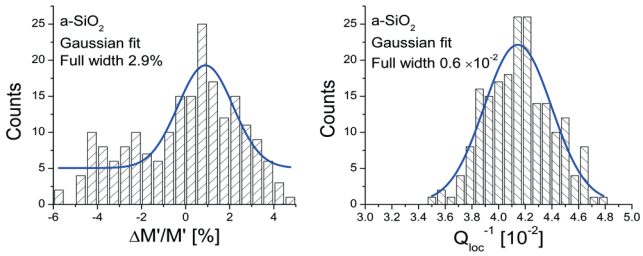

a) b)

Fig. 1. (a): Statistics of the measured indentation modulus on amorphous SiO_2 comprising 200 measuring points. (b): Distribution of internal friction Q_{loc}^{-1} for amorphous SiO_2. Measurements were taken in two maps on 100 different positions in a squared lattice of 200 × 200 nm^2 size

5. Discussion

The variation of AFAM contact-resonance frequencies and hence the local elasticity and local damping of amorphous SiO_2 can be explained in the context of local atomic configuration and atomic-level stress. In disordered materials, there exist large local stresses and prohibit a unique glassy or liquid ground state. Amorphous materials arrange in a large manifold of configurations, in which local stresses vary significantly on the nm-scale [12]. This manifests itself in a potential energy landscape (PEL) which represents in 3N-dimensions a wide variety of metabasins for the amorphous structure in contrast to a single crystalline ground state [12-14]. Each individual metabasin represents a local configuration and can be characterized by its local shear modulus [15]. In other words, there exists a spatially varying relative local modulus $\Delta M'/M'$ and a locally varying internal friction. These effects have been found in the metallic glass PdCuSi as well [2, 6], however, not in the polycrystalline counterpart PdCuSi or the single crystal $SrTiO_3$ which served as materials for comparison [2, 6].

Here, we probe such a structural excitation and/or relaxation locally in Q^{-1}. We observed the same distribution of quantitative

local internal friction as was observed in $\Delta k_r/k_r$ or in $\Delta M'/M'$. Because internal friction by structural relaxation is observed at a subset of metabasins of the potential energy landscape, there exists a locally varying average of relaxation times, which eventually leads to a spatially varying internal friction which we observe here. Recently, combined inelastic X-ray scattering and ultrasonic measurements have revealed that there must be an intrinsic nanoscale inhomogeneity in elasticity [16], which agrees with our arguments presented here.

As in the real part of the modulus, the imaginary part demonstrates the change in the potential energy landscape from the amorphous system into that of the crystalline counterpart. The amorphous PEL has a large variety of metabasins, while the crystalline one has only one metabasin, at least in a single crystal. The width of the distribution gives some insight into the variety of local structures with different local modulus and internal friction values. It proves the variety of a disordered material versus the one of a crystal. Since our measurements with a local probe are limited in spatial resolution to about 10 nm (at a static force of 0.6 μN exerted on the tip) [2], we would expect an even broader distribution if we were able to get a higher resolution in space. Metabasins of local amorphous structures may contain 10 - 1000 atoms, starting from icosahedral clusters up to shear transformation zones, including the Eshelby stress-field [13, 14]. These variations are below the resolution limit of our AFAM-technique. Nevertheless we observe these distributions and can relate them to the structural differences.

In comparison to the metallic glass PdCuSi [2], the distribution in $\Delta M'/M'$ and in Q_{loc}^{-1} [6] is significantly smaller than expected. Since we deal here with a so-called oxide network glass, the distribution of local configurations is limited compared to the metallic glass. Therefore, the distribution of the local modulus and of the local damping is also reduced. This will be explored further in a set of measurements of "fragile" and "strong" glass forming systems.

6. Summary

We demonstrate here a quantitative way to determine the local internal friction or loss on a nanometer scale by using the AFAM-technique. The evaluation of the data is based on the cantilever's mass distribution with damped flexural modes. The width of the distribution changes from the amorphous to the crystalline case as expected from the consequences of the potential energy landscape picture. This is compared to Q_{loc}^{-1} measured in crystalline $SrTiO_3$, which exhibits a narrow distribution, as expected. Future work will concentrate on other amorphous versus crystalline systems like polymers and biopolymers, where the local information on the real and imaginary part of the modulus is most interesting.

Acknowledgement

The authors are grateful for the support of the German Science Foundation within the "Sonderforschungsbereich SFB 1073". B. Zhang acknowledges the support from the AvH foundation and NSF of China (Grant No. 51171055). We thank A. Kumar, Indira Gandhi Centre for Atomic Research, Kalpakkam, India, for helpful discussions.

REFERENCES

[1] L.B. Magalas, Mechanical spectroscopy, internal friction and ultrasonic attenuation.Collection of works, Mater. Sci. Eng. A **521-522**, 405-415 (2009).

[2] H. Wagner, D. Bedorf, S. Küchemann, M. Schwabe, B. Zhang, W. Arnold, K. Samwer, Local elastic properties of a metallic glass, Nature Materials **10**, 439-442 (2011).

[3] F. Marinello, D. Passeri, E. Savio (Eds.), Acoustic Scanning Probe Microscopy, Springer, New York, 2013.

[4] J.J. Vlassak, W.D. Nix, Indentation modulus of elastically anisotropic half-spaces, Phil. Mag. A **67**, 1045-1056 (1993).

[5] P. Yuya, D.C. Hurley, J. A. Turner, Relationship between Q-factor and sample damping for contact resonance atomic force microscope measurement of viscoelastic properties, J. Appl. Phys. **109**, 113528 (2011).

[6] H. Wagner, M. Büchsenschütz-Göbeler, Y. Luo, A. Kumar, W. Arnold, K. Samwer, Measurement of local internal friction in metallic glasses, J. Appl. Phys. **115**, 134307 (2014); Erratum: J. Appl. Phys. **115**, 169902 (2014).

[7] M. Kopycinska-Müller, A. Caron, S. Hirsekorn, U. Rabe, H. Natter, R. Hempelmann, R. Birringer, W. Arnold, Quantitative evaluation of elastic properties of nano-crystalline nickel using atomic force acoustic microscopy, Z. Phys. Chem. **222**, 471-498 (2008).

[8] D.C. Hurley, M. Kopycinska-Müller, A.B. Kos, Mapping mechanical properties on the nanoscale using atomic-force acoustic microscopy, JOM **59**, 23-29 (2007).

[9] G. Stan, R. F. Cook, Mapping the elastic properties of granular Au films by contact resonance atomic force microscopy, Nanotechnology **19**, 23570 (2008).

[10] G. Stan, W. Price, Quantitative measurements of indentation moduli by atomic force acoustic microscopy using a dual reference method, Rev. Sci. Instr. **77**, 103707 (2006).

[11] H. Wagner, Lokale Elastizitätsfluktuationen kristalliner und amorpher Festkörper: Eine experimentelle Vergleichsstudie mittels Ultraschall-Kraftmikroskopie, Diploma Thesis, 1. Phys. Institut, Georg-August Universität Göttingen, 2010, unpublished.

[12] S. Alexander, Amorphous solids: Their structure, lattice dynamics and elasticity, Physics Reports **296**, 65-236 (1998).

[13] F. H. Stillinger, T.A. Weber, Hidden structure in liquids, Phys. Rev. A **25**, 978-989 (1982); F. H. Stillinger, A topographic view of supercooled liquids and glass-formation, Science **31**, 1935-1939 (1995).

[14] J.S. Harmon, M.D. Demetriou, W.L. Johnson, K. Samwer, Anelastic to plastic transition in metallic glass-forming liquids, Phys. Rev. Lett. **99**, 135502 (2007).

[15] W.L. Johnson, K. Samwer, A universal criterion for plastic yielding of metallic glasses with a $(T/T_g)^{2/3}$ temperature dependence, Phys. Rev. Lett. **95**, 195501 (2005).

[16] T. Ichitsubo, H. Kato, E. Matsubara, S. Biwa, S. Hosokawa, K. Matsuda, H. Uchiyama, A.Q. R. Baron, Static heterogeneity in metallic glasses and its correlation to physical properties, J. Non-Crystalline Solids **357**, 494-500 (2011).

Received: 20 October 2015.